Layer-by-Layer Assembly of Inorganic Nanosheets and Polyelectrolytes for Reverse Osmosis Composite Membranes

Jungkyu Choi[1,2], Hyemin Sung[1], Yongmin Ko[1], Seunghye Lee[1], Wanseok Choi[1], Joona Bang[1] and Jinhan Cho[1]

[1] *Department of Chemical and Biological Engineering, Korea University, Anam-dong, Seounguk-gu, Seoul 136-713, Republic of Korea*

[2] *Green School, Korea University, Anam-dong, Seongbuk-gu, Seoul 136-713, Republic of Korea*

Keywords: RO Membrane, Layer-by-Layer Assembly, Electrostatic Interaction, Polyelectrolyte Layers, Montmorillonite (MTM) Nanosheet

In this study, we introduce a layer-by-layer (LbL) assembly method to prepare a reverse osmosis (RO) desalination membrane that consists of a hybrid combination of [polyelectrolyte (PE)/montmorillonite (MTM)]$_n$ layers. First, adopting poly(allylamine hydrochloride) (PAH) for a PE layer, an RO test showed that the permeate flux of water through (PAH/MTM)$_n$ multilayer-coated membranes decreased from ~25.5 to ~8.3 L·m^{-2}·h^{-1} with the increased bilayer number from $n=9$ to $n=18$. At the same time, the corresponding ion rejection with respect to NaCl is increased from ~30 to ~81%. Despite the increased ion rejection performance, (PAH/MTM)$_n$ membranes exhibit a poor chlorine resistance, as frequently observed in commercial polyamide-based RO membranes. In our previous study, it was noted that the RO membranes, prepared just from the PE multilayers (i.e., [PAH/poly(acrylic acid) (PAA)]$_n$ layers), showed a marked chlorine tolerance, but concomitantly very low permeate flux (~4–5 L·m^{-2}·h^{-1}). Considering the significant drawback in each case (poor chlorine tolerance for (PAH/MTM)$_n$ layers and low permeate flux for (PAH/PAA)$_n$ layers), we proposed to combine the layer constituents primarily by inserting PAH/PAA layers between two adjacent PAH/MTM layers. Indeed, the flux is maintained at ~7.5±0.5 L·m^{-2}·h^{-1}, comparable to commercial membranes, while the salt rejection ability is as high as ~75±2.5% and the stability against the chlorine attack is well preserved with ~74±5.0% ion rejection after the NaOCl treatment.

Introduction

Nowadays, one of the most critical problems that mankind faces is a global water shortage. The present fresh water resources are expected to be significantly deficient to meet the future needs for sustainable life. Such inevitable water shortage has led many researchers to develop membrane technologies suitable for producing clean water, for example, via desalting seawater (Shannon *et al.*, 2008; Elimelech and Phillip, 2011). In particular, a reverse osmosis (RO) desalination membrane, which is often composed of polyamide (PA) thin film as a top selective layer, a microporous polysulfone (PSf) support layer, and a nonwoven polyester fabric layer at the bottom, has attracted considerable attention due to its high salt rejection ability (Matsuura, 2001; Khawaji *et al.*, 2008; Lau *et al.*, 2012). Recently, many researchers have focused on developing a novel type for an effective top layer and controlling its micro-structures as desired in order to attain high membrane performance (i.e., permeate flux, salt rejection, and durable stability) (Ulbricht *et al.*, 2002; Zhou *et al.*, 2007; Colquhoun *et al.*, 2010; La *et al.*, 2010; Park *et al.*, 2010). Considering the fact that the performance of an RO desalination membrane is strongly dependent on the physiochemical properties of the top selective layer, appropriate tuning of its surface charge density, porosity, surface roughness, layer structure, and chlorine resistance is of utmost importance towards achieving good performance.

While controlling the properties of the top selective layer, the optimal balance of the resulting membrane performance representatives (i.e., permeate flux, salt rejection, and chlorine resistance) through the top selective layer should be carefully considered to fabricate RO membranes in order to be suitable for practical desalination processes. In particular, PA-based membranes have been widely used to serve as the top selective layer in the commercial RO membrane configuration because of their good salt rejection capability and superior thermal and mechanical properties (Kawai *et al.*, 2004). An increase in the thickness of the PA layer is often beneficial in enhancing the salt rejection, but concomitantly induces an undesirable reduction of the permeate flux. On the contrary, a decrease in the film thickness contributes to increasing the permeate flux, but results in reduced salt rejection. Even if the trade-off between the permeate flux and salt rejection can be well balanced, high chlorine resistance should be secured for practical applications. However, commercially available PA membranes are vulnerable to chlorine, which is generally used as a disinfectant for the prevention of biofouling or as a membrane cleaning agent. Since chlorine attacks the aromatic PA structure, membrane performance can be seriously deteriorated (Tessaro *et al.*,

Received on June 11, 2013; accepted on October 10, 2013
DOI: 10.1252/jcej.13we136
Correspondence concerning this article should be addressed to J. Cho (E-mail address: jinhan71@korea.ac.kr) and J. Bang (E-mail address: joona@korea.ac.kr).

2005; Buch *et al.*, 2008; Khawaji *et al.*, 2008). Therefore, strong demand for alternative RO membranes that also show high performance has been addressed for reliable use in the desalination process, possibly even in the presence of other impurities such as the chlorine. To this end, various materials such as nanoporous polymers, liquid crystals, graphenes, carbon nanotubes, or celluloses have been employed to constitute the single top selective layer instead of the PA layer (Ulbricht *et al.*, 2002; Zhou *et al.*, 2007; Park *et al.*, 2010). Despite the substantial effort of many researchers, to the best of our knowledge, no approaches have successfully allowed for effective control of the permeate flux and salt rejection, while maintaining the high chlorine resistance.

Along with other film fabrication methods such as blending (Ouyang *et al.*, 2004), sol–gel process (Hu *et al.*, 2012), or the self-assembly of block copolymers (Kim *et al.*, 2007), layer-by-layer (LbL) assembly has a high potential to prepare composite films with tailored physicochemical properties. One of the advantages in this approach is that LbL assembly enables the simple, but robust preparation of multi-structured films with an advanced level of control over thickness, composition, and functionality. This was possible through complementary interactions between materials constituting the layers (i.e., electrostatic, hydrogen-bonding or covalent interaction) (Decher, 1997; Podsiadlo *et al.*, 2007). In particular, it was reported that electrostatic LbL-assembled multilayer films obtained by the repetition of depositing oppositely charged polyelectrolytes (PEs) could serve as good ion selective films (Park *et al.*, 2004). However, studies related to the chemical stability of the resulting films under harsh environmental conditions including chlorine attack was not fully conducted in that work. In our previous study (Park *et al.*, 2010), it was noted that the RO membranes comprised of [poly(allylamine hydrochloride]/[poly(acrylic acid)], i.e., PAH/PAA layers allowed for increased chlorine tolerance with ion rejection of ~80% with respect to NaCl, but very low permeate flux (~4–5 $L \cdot m^{-2} \cdot h^{-1}$).

In this study, we also adopted the LbL-assembly as an effective tool for fabricating RO desalination membranes but now with inorganic nanosheets (negatively charged montmorillonite (MTM)) instead of PAA. The use of MTM nanosheets was attempted to provide a facile pathway for water transport through the interface between PAH/MTM layers. Indeed, the increased flux (up to ~9 $L \cdot m^{-2} \cdot h^{-1}$) was observed through the PAH/MTM layers compared to that of PAH/PAA counterparts with comparable ion rejection (~80%) with respect to NaCl. Despite the increased flux, PAH/MTM layers did not preserve the ion rejection after the NaOCl treatment. Therefore, we further employed thermally crosslinked PAH/PAA layers by inserting them between the neighboring PAH/MTM layers in order to secure chemical stability especially against chlorine attack. The resulting $(PAH/PAA/PAH/MTM)_9$ layers showed higher permeate flux (~7.5±0.5 $L \cdot m^{-2} \cdot h^{-1}$) by ~60% compared with that (~4.7±0.7 $L \cdot m^{-2} \cdot h^{-1}$) of the PAH/PAA counterparts with comparable ion rejection (~80%). More importantly, the permeate flux and ion rejection of $(PAH/PAA/PAH/MTM)_9$ layers were well preserved at ~7.8± 0.5 $L \cdot m^{-2} \cdot h^{-1}$ and 74±5.0%, respectively, after the NaOCl treatment, indicating the contribution of crosslinked PAH/PAA layers to the improved chemical stability.

1. Experimental

1.1 Materials

Poly(allylamine hydrochloride) (PAH, M_w = ~120,000–200,000 $g \cdot mol^{-1}$), and poly(acrylic acid) (PAA, M_w = ~100,000 $g \cdot mol^{-1}$) were purchased from Sigma-Aldrich Co. LLC and used as received. Na^+-MTM (Kunimine Industries Co., Ltd.) nanosheets with a cation exchange capacity of 1.15 $meq \cdot g^{-1}$ were used to constitute a continuous layer without further chemical modification. A PSf film (UE50, 100,000 $g \cdot mol^{-1}$, TriSep Corp.) was used as a substrate for supporting a membrane, fabricated by the combination of PAH/MTM and/or PAH/PAA layers.

1.2 LbL assembly for RO membranes

The concentration of both PAH and PAA aqueous solutions was 1 $g \cdot L^{-1}$, while the concentration of MTM suspension in deionized (DI) water was 5 $g \cdot L^{-1}$. The pHs of the PAH solution, PAA solution, and MTM suspension were adjusted to be 7.5, 3.5, and 7.5, respectively. First, the negatively charged PSf substrates (~5.2 cm in diameter) were prepared by soaking in a 0.5 M H_2SO_4 solution at 90°C for 30 min. These substrates were then dipped in the cationic PAH solution for 10 min, and further washed twice in DI water for 1 min. After the deposition of a PAH layer on the PSf substrate, the anionic PAA or MTM was successively deposited onto the PAH layer (dried by nitrogen flow) using the same dipping and washing procedures as described above. The two consecutive depositions of PAH/PAA or PAH/MTM layers resulted in a composite layer, and for convenience, the composite layer is referred to as a bilayer. The deposition of a bilayer was repeated until a desired number (n times) of PAH/PAA or PAH/MTM layers and the resulting layers were denoted as $(PAH/PAA)_n$ and $(PAH/MTM)_n$ layers. In addition, a pair of (PAH/PAA) layers was inserted between the two adjacent (PAH/MTM) layers, constituting (PAH/PAA/PAH/MTM) layers. This deposition step was repeated n times in order to fabricate $(PAH/PAA/PAH/MTM)_n$ layers. The LbL-assembled layers containing (PAH/PAA) layers were thermally annealed at 180°C for 1 h in a vacuum oven. All prepared films were stored in DI water prior to the RO test described below.

1.3 Characterization of LbL-assembled layers

The film thickness and surface morphology of a LbL-assembled membrane were investigated by field-emission scanning electron microscopy (FE-SEM) (S-4300, Hitachi, Ltd.). A quartz crystal microgravimetry (QCM) device (QCM200, SRS, Inc.) was used to monitor the mass change after each deposition step during the membrane fabrication. In particular, the change (ΔF in Hz) of the frequency relative

to the fundamental resonance frequency of the QCM electrode (~5 MHz) was recorded, and it was further converted into the mass change using the Sauerbrey equation.

$$\Delta F = -\frac{2F_0^2}{A\sqrt{\rho_q \mu_q}} \cdot \Delta m \quad (1)$$

Here, F_0 (~5 MHz) is the fundamental resonance frequency of the QCM electrode, A is the electrode area, and ρ_q, (~2.65 g·cm^{-2}) and μ_q (~2.95×10^{11} g·cm^{-2}·s^{-2}) are the density of the quartz and shear modulus, respectively. With the given values, this equation is further simplified as follows.

$$\Delta F = -56.6 \times \Delta m_A \quad (2)$$

It thereby indicates the linear relationship between the frequency change (ΔF in Hz) and mass change per the electrode area (Δm_A in μg·cm^{-2}).

Vibrational spectra were measured by FT-IR spectroscopy (Fourier Transform Infrared Spectroscopy, Nicolet IS10, Thermo Fisher Scientific, Inc.) in the transmission mode. The sample chamber was purged with N_2 gas for 2 h to eliminate water and CO_2 prior to conducting the FT-IR measurement. FT-IR spectra for the (PAH/PAA/PAH/MTM)$_9$ multilayer deposited onto an amorphous Si substrate were obtained from 300 scans. The acquired raw data was plotted after baseline correction and the spectrum was smoothed using spectrum analysis software (OMNIC, Thermo Fisher Scientific, Inc.).

1.4 Membrane performance and chlorine resistance tests

An RO membrane obtained by the above-mentioned layer-by-layer assembly was mounted in a custom-made permeation cell. The effective permeation area was ~13.9 cm^2. The ionic salt (NaCl) concentration and the volumetric feed rate were maintained at ~2,000 ppm and ~0.46 L·h^{-1}, respectively, while the feed side was pressurized to be ~15.5 bar. An outlet at the bottom of the permeation cell was used to collect the permeate solution that passed through the RO membrane. The ion concentration on the permeate side was measured using the ionic conductivity meter (PC650, Eutech Instruments) and the permeate flux was measured by considering the collected permeate amount for a given time. Specifically, the permeate flux (N) and ion rejection (IR) were calculated using the following equations.

$$N = \frac{V}{A_m \cdot t} \quad \text{and} \quad IR\,[\%] = \left(1 - \frac{C_P}{C_F}\right) \times 100 \quad (3)$$

Here, A_m is the membrane area [m^2], V is the permeated amount [L], t is the time [h], and C_F and C_P are the concentrations of salts (NaCl) in the feed and permeation sides, respectively. A schematic for the RO test is illustrated in **Figure 1**.

For the chlorine resistance test, a membrane, prepared by the LbL-assembly, was immersed in a 6,000 ppm NaOCl aqueous solution (pH of 11) for ~1 h, and was further dried at room temperature overnight. Subsequently, the RO test described above was also applied to the chlorine-treated membrane.

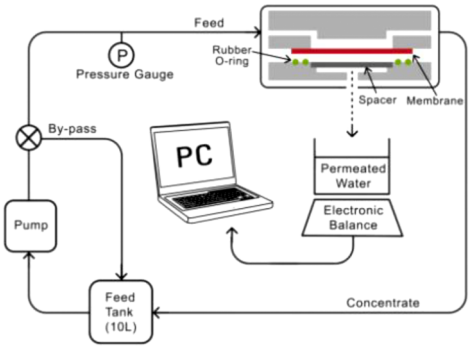

Fig. 1 Schematic diagram of an RO test system

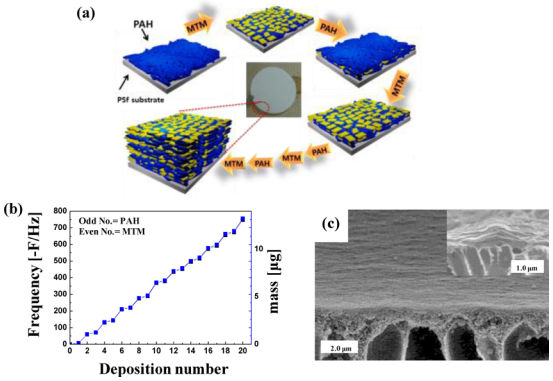

Fig. 2 (a) Schematic illustration for the preparation of LbL-assembled (PAH/MTM)$_n$ multilayers onto PSf substrates; (b) QCM data of (PAH/MTM)$_n$ multilayers as a function of a deposition number; (c) The tilted SEM image of (PAH/MTM)$_n$ multilayer film deposited onto a PSf substrate

2. Results and Discussion

A schematic for an RO desalination membrane prepared by depositing PAH and MTM nanocomposite layers onto a PSf substrate via the electrostatic LbL-assembly is depicted in **Figure 2(a)**. In particular, a positively charged PAH layer was first formed on the negatively charged PSf substrate and further served as a basis for forming the next negatively charged MTM layer. PAH was alternately LbL-assembled with MTM sheets via electrostatic interactions between cationic amine groups (–NH_3^+) of PAH and anionic surface groups (≡Si–O^-) of MTM (Celis *et al.*, 2000; Podsiadlo *et al.*, 2007).

These electrostatic layers were alternately deposited onto the PSf substrate to a desired number (n) of the (PAH/MTM)$_n$ multilayers. The growth of composite layers via the alternating depositions of the PAH and MTM layers was quantitatively monitored by tracing the frequency change in QCM. Figure 2(b) shows the frequency changes (ΔF in Hz) and the corresponding mass changes (Δm_A in μg·cm^{-2}) per membrane area as a function of the number of deposition steps. These results indicate that each layer, formed from the PAH solution or MTM suspension, contributed to

increasing the mass of the composite film. Specifically, the one-time depositions by the PAH solution and the MTM suspension resulted in the change of frequencies, $-\Delta F$ of ~19 and ~74 Hz, respectively, which were equivalent to the mass change per membrane area, Δm_A of ~0.34 and ~1.28 $\mu g \cdot cm^{-2}$, respectively. In addition, the cross-sectional SEM image of Figure 2(c) indicates that 18 repetitions of the deposition of the PAH/MTM layer, i.e., $(PAH/MTM)_{18}$ multilayer resulted in ~250 nm, suggesting that a ~10–15 nm thick layer was formed due to the bilayer deposition.

Additionally, the vibrational spectroscopic characterizations of pristine and thermally annealed PAH/MTM films were investigated using FT-IR spectroscopy in an attempt to assess the thermal stability of PAH/MTM films (see **Figure A1**). The FT-IR characterization revealed that the electrostatic bonding (or interaction) formed at the interfaces of PAH and MTM layers was not chemically influenced by thermal annealing at 180°C, indicating the high thermal stability of PAH/MTM interfaces.

When these nanocomposite films are used as desalination RO membranes, the ability to control their film thickness especially via the appropriate choice of the bilayer number allows tuning of the corresponding desalination performance as reflected by the permeate flux and salt rejection. In order to see the effect of the bilayer number (i.e., film thickness) on performance, the desalination performance of $(PAH/MTM)_n$ layers was investigated with increasing the bilayer number (n) from 9 to 18 (**Figure 3**). With the increase in the bilayer number, the permeate flux of the composite films were monotonically decreased from ~25.5 (for $n=9$) through ~15.2 and ~10.5 (for $n=12$ and for $n=15$, respectively) to ~8.3 $L \cdot m^{-2} \cdot h^{-1}$ ($n=18$), while the salt rejection rather kept increasing from ~30 (for $n=9$) through ~56 and ~79 (for $n=12$ and for $n=15$, respectively) to ~81% (for $n=18$). The conventional trade-off relationship between the permeate flux and ionic rejection (Geise *et al.*, 2011) was observed for these $(PAH/MTM)_n$ layers as well. This phenomenon indicates that the increase in the film thickness of a multilayer, comprised of a pair of PAH/MTM layers, was beneficial in enhancing the salt rejection at the expense of the inevitable decrease in the permeate flux, seemingly due to the longer diffusion pathway along the film thickness.

However, the marked desalination performance of these $(PAH/MTM)_n$ films was significantly reduced after the chlorine treatment with the NaOCl solution. For example, the permeate flux through $(PAH/MTM)_{18}$ layers was increased from ~9.0±0.7 to ~20±1.1 $L \cdot m^{-2} \cdot h^{-1}$ and the ion rejection was decreased from ~79±2.3 to ~54±6.2% (**Figure 4(a)**). It was reported that the chlorine in the feed can cause the ring-chlorination reaction through an intramolecular rearrangement of a chlorine atom into the aromatic ring, and thus the degradation of a membrane (Misdan *et al.*, 2012). Considering the fact that the PAH/MTM layers in this study do not contain an aromatic ring structure, the effect of NaOCl treatment on the desalination performance of PAH/MTM layers could be presumably attributed to the

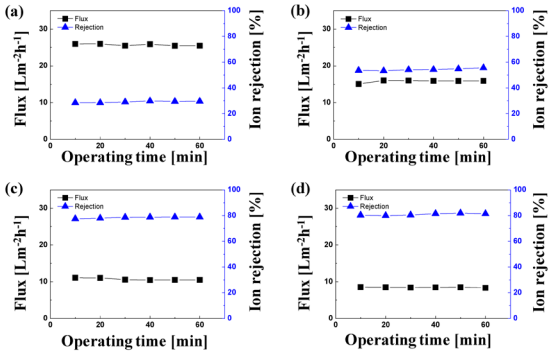

Fig. 3 Permeate flux and ion rejection as a function of operation time for $(PAH/MTM)_n$ multilayers; (a) $n=9$, (b) $n=12$, (c) $n=15$, and (d) $n=18$

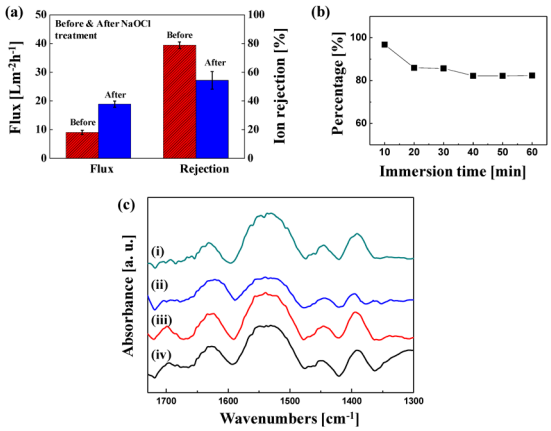

Fig. 4 (a) Plot of permeate flux and ion rejection for $(PAH/MTM)_{18}$ multilayers before and after the NaOCl treatment for 1 h; (b) Normalized mass change of $(PAH/MTM)_{18}$ multilayers as a function of the immersion time in the NaOCl solution; (c) FT-IR spectra of $(PAH/PAA/PAH/MTM)_9$ multilayers (i) before and (ii) after thermal annealing at 180°C, and (iii and iv) after an additional immersion of sample (ii) in (iii) the NaCl solution (pH 8.1) and (iv) the NaOCl solution (pH 11)

high pH value (~11) and/or the concentration (6,000 ppm) of the NaOCl solution. Generally, it is well known that the film structural stability of LbL layers, composed of cationic amine-based PEs and oppositely charged counterparts, is sensitive to the solution pH and ionic salt concentration (Mendelsohn *et al.*, 2000). It was previously reported that the pK_a of the amine-functionalized polymers is 9.0 and the amino groups are almost neutralized at pH 11 (Choi and Rubner, 2005). Therefore, PAH/MTM multilayers assembled at pH 7.5 can be destabilized by inducing the dissociation of electrostatic bonds due to the conversion from protonated amine to uncharged amine groups in a NaOCl solution of pH 11. Additionally, the presence of concentrated ionic species plausibly weakens the electrostatic interaction between the contacting oppositely charged layers. For example, it was reported that anionic PAA/cationic poly(diallyldimethylammonium) multilayers are rapidly removed at salt concentrations greater than 0.6 M NaCl (Dubas *et al.*, 2001). Nevertheless, it was reported

that a charged polyelectrolyte (PE) layer embedded within electrostatic LbL multilayers, equivalent to PAH/MTM films in this study, has a relatively higher degree of ionization than the spin-casted film composed of single PE species due to the charge inducing effect by oppositely charged PE layer (Choi and Rubner, 2005). Therefore, PAH and/or MTM layers were not likely to be totally delaminated in the NaOCl solution used in this study. Instead, the chlorine treatment at both high pH and ionic concentration would lead to partial swelling and destabilization of the (PAH/MTM) layers, thereby allowing for the facile diffusion of salts and concomitant lowered salt rejection. These postulations were supported by the partial loss in the mass of a $(PAH/MTM)_{18}$ layer after its immersion in the NaOCl solution (**Figure 4(b)**).

Taking into account the barrier property of inorganic MTM sheets with respect to salts, cationic PEs have been employed along with the MTM sheets in an attempt to fabricate composite films with a periodic organic/inorganic structure analogous to a nacre-like structure (Podsiadlo *et al.*, 2007, 2008). Podsiadlo *et al.* (2008) reported that the structure of composite films, composed of poly(ethyleneimine) (PEI), PAA, and MTM, could not avoid the fast diffusion/reptation of PEs through the space among MTM sheets during the "in-and-out" diffusion of polymer. These results imply that the MTM layers within composite films had much difficulty in forming a dense structure incorporated with the PEI layer and, therefore, in serving as an effective barrier layer. A similar scenario can be employed to explain the poor membrane performance of the chlorine-treated $(PAA/MTM)_n$ composite membranes in this study.

To improve the chlorine resistance of PAH/MTM layers while maintaining the high desalination performance, a thermally crosslinkable (PAH/PAA) bilayer was periodically inserted between two adjacent (PAH/MTM) layers. By using this scheme and repeating the deposition steps 9 times, we synthesized a $(PAH/PAA/PAH/MTM)_9$ composite layer having a film thickness comparable to that ($\sim$250 nm) of $(PAH/MTM)_{18}$ multilayers. As reported in a number of precedent work (Mendelsohn *et al.*, 2000; Zhai *et al.*, 2004), the LbL assembly of the PAH and PAA solutions with the pHs of 7.5 and 3.5, respectively, induces a chain conformation with abundant loops and tails. In a PAA solution at pH 3.5, weakly ionized PAA chains (pK_a of PAA: $\sim$4.5) with a number of loop and coil structures are deposited onto almost a fully charged PAH layer (pK_a of PAH: $\sim$9.0) (Choi and Rubner, 2005). On the contrary, when the PAH chains are deposited on a PAA layer at pH 7.5, the weakly ionized carboxylic acid groups of the pre-formed PAA layer are converted into a highly ionized state (i.e., COO^-). Therefore, a large amount of PAH chains containing positively charged amine groups are required to neutralize the ionized surface of the PAA layer and realize charge reversal via charge overcompensation. As a result, the depositions of PAH at pH 7.5 and PAA at pH 3.5 for constituting $(PAH/PAA/PAH/MTM)_9$ multilayers apparently contained a high degree of unbound carboxylic acid and amine groups as well as a number of internal charge pairing groups. In view of the RO membrane, these phenomena are very important to determine the final film structure because internal charge pairing groups can be chemically crosslinked via the amide bonding during thermal treatment and, furthermore, a large amount of unbound carboxylic acid and amine groups can provide seawater desalination membranes with efficient ion rejection. That is, the introduction of thermally crosslinked PAH/PAA layers into PAH/MTM films, allowing a strong, dense structural property in the final composite films, can significantly improve the membrane stability especially against degradation due to the chlorine attack.

To verify this hypothesis, residual carboxylic acid and amine groups in the $(PAH/PAA/PAH/MTM)_9$ layers were identified using FT-IR spectroscopy. As shown in **Figure 4(c)**, the FT-IR spectra of the multilayers before the thermal treatment revealed the presence of $-COO^-$ (carboxylate peak at 1,570 and 1,390 cm^{-1}), –COOH (free acid peak at 1,700 cm^{-1}), $-NH_3^+$ (symmetric and antisymmetric NH_3^+ deformation between 1,625 and 1,400 cm^{-1}), and $-NH_2$ (N–H scissor bending at 1,630 and 1,550 cm^{-1}). When the multilayers were thermally annealed at 180°C, the absorbance peak intensity at 1,700 and 1,630 cm^{-1} was increased due to the partial formation of amide group indicating the cross-linkage between the carboxyl acid and amine groups (the absorbance peak of amide groups at 1,700 cm^{-1} was overlapped with that of –COOH group) ((ii) in Figure 4(c)). After immersing these films in the aqueous media at pH 8.1 (similar to that of the seawater solution), the absorption peaks of $-COO^-$ groups at 1,560 and 1,390 cm^{-1} were more evident compared to that of thermally annealed multilayers ((iii) in Figure 4(c)). These phenomena were still observed after applying chlorine treatment to the crosslinked $(PAH/PAA/PAH/MTM)_9$ multilayers ((iv) in Figure 4(c)). However, we did not detect the degradation of the amide bonding formed between PAH and PAA within multilayers. These results show the possibility that the crosslinked $(PAH/PAA/PAH/MTM)_n$ films can maintain the highly charged state in seawater of pH 8.1 and, furthermore, can be effectively used as a desalination membrane with a high level of chemical stability.

Based on these results, we measured the desalination performance of a crosslinked $(PAH/PAA/PAH/MTM)_9$ multilayer (a schematic fabrication process is shown in **Figure 5(a)**) before and after chlorine treatment (**Figure 5(b)**). Interestingly, the desalination performance of the crosslinked membrane remained almost unchanged, implying a high resistance against chlorine attack. Furthermore, the permeate flux ($\sim 7.8 \pm 0.2\,L \cdot m^{-2} \cdot h^{-1}$) and ion rejection ($\sim 74 \pm 5.0\%$) through the crosslinked membrane after chlorine treatment were quite comparable to those ($\sim 9.0 \pm 0.7\,L \cdot m^{-2} \cdot h^{-1}$ and $\sim 79 \pm 2.3\%$) obtained through $(PAH/MTM)_{18}$ multilayers before chlorine treatment. Although a $\sim$250 nm thick multilayer, mainly comprised of PAH and PAA layers, exhibited a similar ion rejection of $\sim 78 \pm 3.6\%$ with a high degree of chlorine stability, the permeate flux ($\sim 4.4 \pm 0.8\,L \cdot m^{-2} \cdot h^{-1}$)

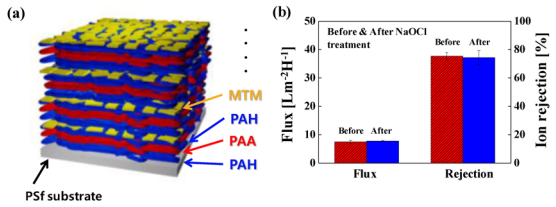

Fig. 5 (a) Schematic of the alternating depositions of PAH/PAA and PAH/MTM layers and (b) permeate flux and salt rejection of thermally annealed $(PAH/PAA/PAH/MTM)_9$ multilayers before and after the NaOCl treatment

of PAH/PAA-based films after chlorine treatment was lower than that ($\sim 7.8 \pm 0.2\,L \cdot m^{-2} \cdot h^{-1}$) of PAH/PAA/PAH/MTM-based counterparts. This suggests that the film structure of PAH/PAA multilayers was denser than that of PAH/PAA/PAH/MTM multilayers. At this point, we would like to point out that although pure PAH/MTM layers were vulnerable to chlorine attack, the MTM sheets in the $(PAH/PAA/PAH/MTM)_9$ multilayer were stabilized by the thermally crosslinked PAH/PAA/PAH layers, which showed a good chlorine resistance themselves.

As mentioned earlier, it has been demonstrated by Podsiadlo *et al.* (2008) that PE layers embedded within $(PEI/MTM/PEI/PAA)_n$ multilayers are seriously interdigitated between oppositely charged PE chains through the openings between MTM sheets. Considering this previous report, MTM sheets within the annealed PAH/PAA/PAH/MTM multilayers are surrounded by thermally crosslinked PAH/PAA/PAH layers, and resultantly these films can be stabilized without any delamination phenomenon during NaOCl treatment. In order to demonstrate this possibility, we further measured the QCM data of thermally crosslinked PAH/PAA/PAH/MTM multilayers by varying the immersion time in NaOCl solution. As shown in **Figure A2**, we did not observe any loss of adsorbed materials, supporting the structural stability of the annealed PAH/PAA/PAH/MTM multilayers. Thus, $(PAH/PAA/PAH/MTM)_n$ multilayers can maintain high ionic rejection performance. Considering that most membranes show a trade-off relationship between the permeate flux and salt rejection (Geise *et al.*, 2011), the combination of inorganic nanosheet layers and thermally crosslinked PE layers without the aromatic ring structure is effective for the preparation of RO membranes, and thus for the flexible adjustment of performance via the appropriate choice of the film constituent (related to the film structure) and the deposition number (related to the film thickness).

Conclusion

In conclusion, we have prepared an RO desalination membrane based on the electrostatic LbL-assembly of inorganic MTM nanosheets/PE multilayers. The salt rejection in $(PAH/MTM)_n$ multilayered membrane increased from ~ 30 to $\sim 81\%$; whereas, the permeate flux decreased from ~ 25.5 to $\sim 8.3\,L \cdot m^{-2} \cdot h^{-1}$ with the increased bilayer number from $n = 9$ to $n = 18$. However, $(PAH/MTM)_n$ multilayers did not preserve the ionic rejection capacity after chlorine treatment, indicating the poor chemical stability plausibly in high pH and/or concentration conditions.

As complementary to the PAH/MTM layers, the periodic insertion of the thermally crosslinked PAH/PAA bilayer between the two adjacent PAH/MTM bilayers contributed to improving the chemical stability of the final composite membranes against the chlorine attack (the permeate flux up to $\sim 7.8 \pm 0.2\,L \cdot m^{-2} \cdot h^{-1}$, and the salt rejection up to $74 \pm 5.0\%$ after the chlorine treatment). Although much more effort in developing a novel membrane technology is still required to achieve high desalination performance, we believe that our approach can provide useful guidance to the rational design of an appropriate film structure, especially the selective top layer.

Acknowledgement

This work was supported by National Research Foundation (NRF) grant funded by the Korea Government (Ministry of Science, ICT & Future Planning) (2010-0029106), and also supported by the Human Resources Development Program (No. 20134010200600) of the Korea Institute of Energy Technology Evaluation and Planning (KETEP) grant funded by the Korea government Ministry of Trade, Industry and Energy.

Literature Cited

Buch, P. R., D. Jagan Mohan and A. V. R. Reddy; "Preparation, Characterization and Chlorine Stability of Aromatic–Cycloaliphatic Polyamide Thin Film Composite Membranes," *J. Membr. Sci.*, **309**, 36–44 (2008)

Celis, R., M. C. Hermosin and J. Cornejo; "Heavy Metal Adsorption by Functionalized Clays," *Environ. Sci. Technol.*, **34**, 4593–4599 (2000)

Choi, J. and M. F. Rubner; "Influence of the Degree of Ionization on Weak Polyelectrolyte Multilayer Assembly," *Macromolecules*, **38**, 116–124 (2005)

Colquhoun, H. M., D. Chappell, A. L. Lewis, D. F. Lewis, G. T. Finlan and P. J. Williams; "Chlorine Tolerant, Multilayer Reverse-Osmosis Membranes with High Permeate Flux and High Salt Rejection," *J. Mater. Chem.*, **20**, 4629–4634 (2010)

Decher, G.; "Fuzzy Nanoassemblies: toward Layered Polymeric Multicomposites," *Science*, **277**, 1232–1237 (1997)

Dubas, S. T., T. R. Farhat and J. B. Schlenoff; "Multiple Membranes from "True" Polyelectrolyte Multilayers," *J. Am. Chem. Soc.*, **123**, 5368–5369 (2001)

Elimelech, M. and W. A. Phillip; "The Future of Seawater Desalination: Energy, Technology, and the Environment," *Science*, **333**, 712–717 (2011)

Geise, G. M., H. B. Park, A. C. Sagle, B. D. Freeman and J. E. McGrath; "Water Permeability and Water/Salt Selectivity Tradeoff in Polymers for Desalination," *J. Membr. Sci.*, **369**, 130–138 (2011)

Hu, L. C., Y. Yonamine, S. H. Lee, W. E. van der Veer and K. J. Shea; "Light-Triggered Charge Reversal of Organic-Silica Hybrid Nanoparticles," *J. Am. Chem. Soc.*, **134**, 11072–11075 (2012)

Kawai, T., C. Ohtsuki, M. Kamitakahara, T. Miyazaki, M. Tanihara, Y. Sakaguchi and S. Konagaya; "Coating of an Apatite Layer on Polyamide Films Containing Sulfonic Groups by a Biomimetic Process," *Biomaterials*, **25**, 4529–4534 (2004)

Khawaji, A. D., I. K. Kutubkhanah and J.-M. Wie; "Advances in Seawater Desalination Technologies," *Desalination*, **221**, 47–69 (2008)

Kim, B. J., J. Bang, C. J. Hawker, J. J. Chiu, D. J. Pine, S. G. Jang, S. M. Yang and E. J. Kramer; "Creating Surfactant Nanoparticles for Block Copolymer Composites through Surface Chemistry," *Langmuir*, **23**, 12693–12703 (2007)

La, Y. H., R. Sooriyakumaran, D. C. Miller, M. Fujiwara, Y. Terui, K. Yamanaka, B. D. McCloskey, B. D. Freeman and R. D. Allen; "Novel Thin Film Composite Membrane Containing Ionizable Hydrophobes: pH-Dependent Reverse Smosis Behavior and Improved Chlorine Resistance," *J. Mater. Chem.*, **20**, 4615–4620 (2010)

Lau, W. J., A. F. Ismail, N. Misdan and M. A. Kassim; "A Recent Progress in Thin Film Composite Membrane: A Review," *Desalination*, **287**, 190–199 (2012)

Matsuura, T.; "Progress in Membrane Science and Technology for Seawater Desalination—A Review," *Desalination*, **134**, 47–54 (2001)

Mendelsohn, J. D., C. J. Barrett, V. V. Chan, A. J. Pal, A. M. Mayes and M. F. Rubner; "Fabrication of Microporous Thin Films from Polyelectrolyte Multilayers," *Langmuir*, **16**, 5017–5023 (2000)

Misdan, N., W. J. Lau and A. F. Ismail; "Seawater Reverse Osmosis (SWRO) Desalination by Thin-Film Composite Membrane—Current Development, Challenges and Future Prospects," *Desalination*, **287**, 228–237 (2012)

Ouyang, J. Y., C. W. Chu, C. R. Szmanda, L. P. Ma and Y. Yang; "Programmable Polymer Thin Film and Non-Volatile Memory Device," *Nat. Mater.*, **3**, 918–922 (2004)

Park, M.-K., S. Deng and R. C. Advincula; "pH-Sensitive Bipolar Ion-Permselective Ultrathin Films," *J. Am. Chem. Soc.*, **126**, 13723–13731 (2004)

Park, J., J. Park, S. H. Kim, J. Cho and J. Bang; "Desalination Membranes from pH-Controlled and Thermally-Crosslinked Layer-by-Layer Assembled Multilayers," *J. Mater. Chem.*, **20**, 2085–2091 (2010)

Podsiadlo, P., A. K. Kaushik, E. M. Arruda, A. M. Waas, B. S. Shim, J. Xu, H. Nandivada, B. G. Pumplin, J. Lahann, A. Ramamoorthy and N. A. Kotov; "Ultrastrong and Stiff Layered Polymer Nanocomposites," *Science*, **318**, 80–83 (2007)

Podsiadlo, P., M. Michel, J. Lee, E. Verploegen, N. Wong Shi Kam, V. Ball, J. Lee, Y. Qi, A. J. Hart, P. T. Hammond and N. A. Kotov; "Exponential Growth of LBL Films with Incorporated Inorganic Sheets," *Nano Lett.*, **8**, 1762–1770 (2008)

Shannon, M. A., P. W. Bohn, M. Elimelech, J. G. Georgiadis, B. J. Marinas and A. M. Mayes; "Science and Technology for Water Purification in the Coming Decades," *Nature*, **452**, 301–310 (2008)

Tessaro, I. C., J. B. A. da Silva and K. Wada; "Investigation of Some Aspects Related to the Degradation of Polyamide Membranes: Aqueous Chlorine Oxidation Catalyzed by Aluminum and Sodium Laurel Sulfate Oxidation during Cleaning," *Desalination*, **181**, 275–282 (2005)

Ulbricht, M., M. Belter, U. Langenhangen, F. Schneider and W. Weigel; "Novel Molecularly Imprinted Polymer (MIP) Composite Membranes via Controlled Surface and Pore Functionalizations," *Desalination*, **149**, 293–295 (2002)

Zhai, L., F. C. Cebeci, R. E. Cohen and M. F. Rubner; "Stable Superhydrophobic Coatings from Polyelectrolyte Multilayers," *Nano Lett.*, **4**, 1349–1353 (2004)

Zhou, M., P. R. Nemade, X. Lu, X. Zeng, E. S. Hatakeyama, R. D. Noble and D. L. Gin; "New Type of Membrane Material for Water Desalination Based on a Cross-Linked Bicontinuous Cubic Lyotropic Liquid Crystal Assembly," *J. Am. Chem. Soc.*, **129**, 9574–9575 (2007)

Appendix

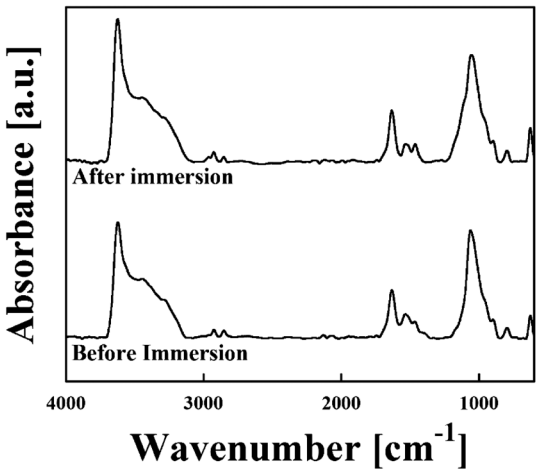

Fig. A1 FT-IR spectra of pristine and thermally annealed PAH/MTM multilayers

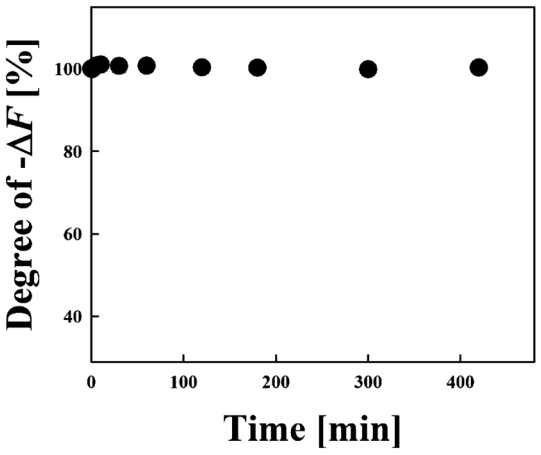

Fig. A2 Normalized frequency (or mass) change of thermally annealed $(PAH/PAA/PAH/MTM)_9$ multilayers as a function of the immersion time in the NaOCl solution